ISSN 1 746-7233, England, UK
World Journal of Modelling and Simulation
Vol. 9 (2013) No. 4, pp. 277-288

Lattice boltzmann simulation of laminar flow in a three-dimensional two-sided lid-driven cavity

Arumuga Perumal*

Department of Mechanical Engineering, V.V. College of Engineering, Thisaiyanvilai, Tamilnadu-628657, India

(*Received February 14 2013, Revised May 25 2013, Accepted September 18 2013*)

Abstract. The present paper computes the laminar flow in a three-dimensional two-sided lid-driven cubical cavity by lattice Boltzmann method. It is known that, the development of Lattice Boltzmann Method is the promising method that uses different kind of non-conventional techniques for applications in computational fluid dynamics. In the present work, the performance and accuracy of the code is first ascertained by computing the flow in a single-sided lid-driven cubical cavity and comparing the results available in the literature. It is found that antiparallel motion of the two-sided lid-driven cubical cavity walls, there appears a single primary vortex with its centre in the centre of the domain. The results for the parallel motion of the walls are also presented in some detail. The problem therefore merits careful investigation, which is attempted in this paper through the lattice Boltzmann method for various Reynolds numbers for the antiparallel and parallel motion of the walls.

Keywords: Lattice Boltzmann method, two-sided lid-driven cubical cavity, D2Q9 model, D3Q19 model, antiparallel wall motion, parallel wall motion

1 Introduction

Aircraft configurations include cavities as an integral part of design, manufacture and performance. Cavity flow is a topical research field relevant to aeroacoustics (noise generation) and transition studies[19]. The present two-sided lid-driven cavity problem is also attractive because of its importance in industrial applications such as coating & drying technologies, melt spinning processes and many others[15]. During the last few decades, both experimental and computational studies have been conducted into the lid-driven square cavity-flow physics[5]. Although there have been some studies considering incompressible cubical cavity flow, these were mainly focused on flow inside a three-dimensional single-sided lid-driven cubical cavity flow[3]. It is also known that, numerical simulations for the single-sided lid-driven cavity flow have been studied by many authors using conventional numerical schemes such as finite difference, finite volume and finite element methods only[11, 20]. Recently, Beya and Lili[4] numerically solved the three-dimensional two-sided non-facing lid-driven cavity flows for various Reynolds numbers using projection method with multigrid technique.

In the past few years, a different kind of numerical method for applications in CFD, namely, the Lattice Boltzmann Method (LBM) has gained popularity[1]. The LBM has emerged as a new effective and alternative approach of CFD and it has achieved considerable success in simulating fluid flows and heat transfer problems[7, 12, 18]. In the LBM approach, one solves the kinetic equation for the particle distribution function. The macroscopic variables such as velocity, temperature and pressure are obtained by evaluating the hydrodynamic moments of the particle distribution function[8]. One of the most popular and simple approaches in the LBM is lattice Boltzmann equation with linearized collision operator based on the Bhatnagar-Gross-Krook (LBGK) collision model[6].

* Corresponding author. Tel.: +91 9159860535.
E-mail address: d.perumal@iitg.ernet.in.

The majority of the LBM works so far dealt with two-dimensional flows. A few researchers have carried out simulations of the single-sided cubical cavity flow using LBM. Limited number of reliable numerical results for steady state three-dimensional single-sided cubical cavity results has been obtained by LBM in the past few years[2, 9, 21]. The lattice Boltzmann simulation of single-sided lid-driven cubical cavity flow was performed by Mei et al.[17]. Furthermore, in contrast to the fairly large number of studies conducted for single-sided lid-driven cavities, only a few investigations have been carried out for flows in two-dimensional two-sided lid-driven cavities by continuum-based methods[13, 14] and no attempt has been made to compute the flow in a two-sided lid-driven cubical cavity with various Reynolds number by LBM.

This paper is organized in four sections. In Section 2, Lattice Boltzmann method and three-dimensional nineteen-velocity lattice model is described in some detail. The two-dimensional nine-velocity square lattice is also described in this section. In Section 3, the three-dimensional two-sided lid-driven cubical cavity problems are described and the results with antiparallel and parallel motion of the walls are presented. Concluding remarks are made in Section 4.

2 Lattice boltzmann method

The Lattice Boltzmann equation which can be linked to the Boltzmann equation in kinetic theory is formulated as [18]

$$f_i(x + c_i, t + \Delta t) - f_i(x, t) = \Omega_i,\ i = 0, 1, \cdots, N, \tag{1}$$

where f_i is the particle distribution function, c_i is the particle velocity along the ith direction and Ω_i is the collision operator. The lattice Boltzmann method with single time relaxation is given by [7]

$$f_i(x + c_i, t + \Delta t) - f_i(x, t) = -\frac{1}{\tau}[f_i(x, t) - f_i^{eq}(x, t)]\ i = 0, 1, \cdots, N. \tag{2}$$

Here f_i^{eq} is the equilibrium distribution function at x, t and τ is the time relaxation parameter.

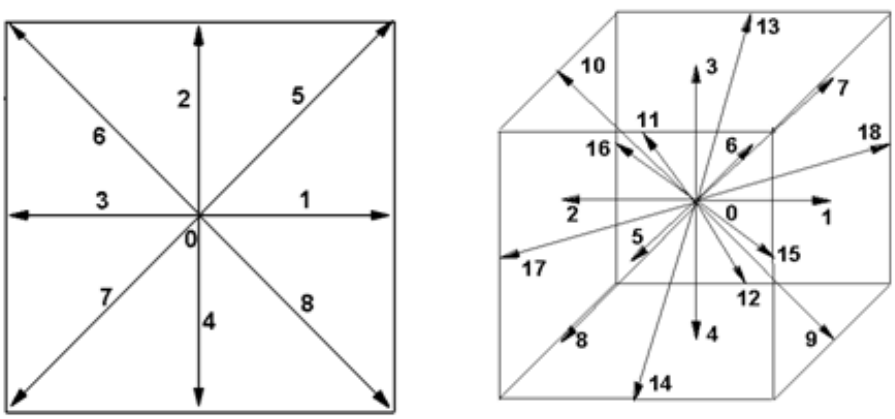

Fig. 1. (a) Two-Dimensional nine-velocity square lattice model. (b) Three-dimensional nineteen-velocity cubic lattice model

For simulating 2D flows, the nine-velocity model (D2Q9, $i = 0, 1, \cdots, 8$) and for simulating 3D flows, the nineteen-velocity model (D3Q19, $i = 0, 1, \cdots, 8$) is used in this work (Fig. 1). All the above LBE models have a rest particle in the discrete velocity set c_i, because the LBE models with a rest particle have better computational stability and reliability. For the D_2Q_9 model the discrete velocity set c_i is written as [15]

$$c_i = \begin{cases} (0,0), & i = 0; 7 \quad \text{group } 0, \\ (\pm 1, 0), (0, \pm 1), & i = 1, 2, 3, 4; \quad \text{group } I, \\ (\pm 1, 1), & i = 5, 6, 7, 8; \quad \text{group } II. \end{cases} \tag{3}$$

and the lattice weights are

$$w_i = \begin{cases} 4/9, & i = 0, \\ 1/9, & i = 1, 2, 3, 4, \\ 1/36, & i = 5, 6, 7, 8. \end{cases} \tag{4}$$

For the D_3Q_19 model the discrete velocity set c_i can be expressed as [7]

$$c_i = \begin{cases} (0,0,0), & i = 0; & \text{group } 0, \\ (\pm 1, 0), (0, \pm 1, 0), (0, 0, \pm 1), & i = 1, 2, \cdots, 6; & \text{group } I, \\ (\pm 1, \pm 1, 0), (\pm 1, 0, \pm 1), (0, \pm 1, \pm 1), & i = 7, 8, \cdots, 18; & \text{group } II. \end{cases} \tag{5}$$

and the lattice weights are

$$w_i = \begin{cases} 2/9, & i = 0, \\ 1/18, & i = 1, 2, \cdots, 6, \\ 1/36, & i = 7, 8, \cdots, 18. \end{cases} \tag{6}$$

In the above, group 0 indicates a rest particle, group I is for the links pointing to the nearest neighbours, group II is for the links pointing to the next-nearest neighbours. The equilibrium distribution functions $f_i^{eq}(x,t)$, for all of the above models which can be expressed in the form as [7].

$$f_i^{(eq)} = \rho w_i \Big[1 + 3(c_i.u) + 4.5(c_i.u)^2 - 1.5(u.u) \Big]. \tag{7}$$

The macroscopic quantities such as density ρ and momentum density ρu are defined in terms of the particle distribution function f_i as follows:

$$\rho = \sum_{i=0}^{N} f_i, \ \rho u = \sum_{i=0}^{N} f_i c_i. \tag{8}$$

The relaxation time τ that fixes the rate of approach to equilibrium is related to the kinematic viscosity υ by [16]

$$\tau = \frac{6\upsilon + 1}{2}. \tag{9}$$

where υ is the kinematic viscosity measured in lattice units. It is seen that $\tau = 0.5$ is the critical value for ensuring a non-negative kinematic viscosity. Numerical instability can occur for a τ close to this critical value. Boundary Conditions and initial conditions are essential for any computational fluid dynamic methods. In LBM several boundary conditions have been proposed[18]. Implementation of boundary conditions in LBM is an important task owing to the fact that one has to translate given information from macroscopic variables to particle distribution function (f_i), since it is the only variable to be evaluated in LBM. To ensure the no-slip boundary condition ($U = 0$) on the wall, Yu et al.[7] suggested a improved bounce-back boundary condition using a linear interpolation formula

$$f_{\tilde{i}}(x_w) = f_{\tilde{i}}(x_w) + \frac{\Delta}{1 + \Delta} \Big(f_{\tilde{i}}(x_f + c_i) - f_{\tilde{i}}(x_w) \Big). \tag{10}$$

The above boundary condition is valid for both $\Delta < 0.5$ and $\Delta \geq 0.5$. For a moving wall Yu et al.[7] added additional momentum

$$f_{\tilde{i}}(x_w, t + \Delta t) = f_i(x_w, t + \Delta t) + 2 w_i \rho \frac{3}{c^2} c_i.u_w, \tag{11}$$

where $f_{\tilde{i}}$ indicates post-collision state. A lid-velocity of $U = 0.1$ has been considered in this work. Since Mach number is U/c_s, where c_s equals $1/\sqrt{3}$ a Mach number of 0.1732, well within the incompressible

limit, is obtained. The velocities are assumed to be zero at the time of starting the simulations for all nodes. Initially, the equilibrium particle distribution function that corresponds to the flow-variables is assumed as the unknown distribution function for all node at $t = 0$. Also a uniform fluid density $\rho = 1.0$ is imposed initially. All the present results obtained in this work are normalized by the top velocity U. The solution procedure of the LBM models at each time step comprise streaming and collision step, application of boundary conditions, calculation of particle distribution function followed by calculation of macroscopic variables. The convergence criterion for all computations was set as

$$\frac{\sum \left(u_{i,j,k}^{n+1} - u_{i,j,k}^{n} \right)^2}{\sum \left(u_{i,j,k}^{n+1} \right)^2} \leq 10^{-6}. \tag{12}$$

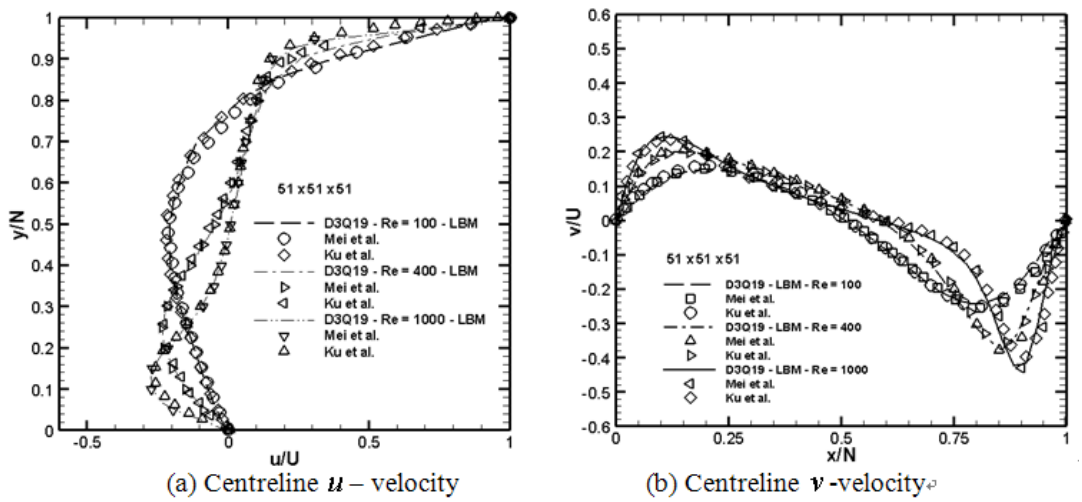

(a) Centreline u – velocity (b) Centreline v -velocity

Fig. 2. Comparison of centreline velocities of a single-sided lid-driven cubical (mid-span) cavity at Re = 100, 400 and 1000

3 Results and discussion

3.1 Code validation

First, the developed LBM code is used to compute the single-sided lid-driven cubical cavity flow for $Re = 100, 400$ and 1000 on a $51 \times 51 \times 51$ lattice size. It is known that, the cubical cavity is the three-dimensional analogue of the square cavity problem. Initially the three-dimensional incompressible laminar single-sided lid-driven flow in a cubical cavity is computed through the developed LBM code for code validation exercise and to show the performance of LBM. Fig. 1 shows the variation of u-velocity along the vertical centreline and v-velocity along the horizontal centreline on the $z = 0.5$ plane (i.e. mid-span) at $Re = 100, 400$ and 1000. The agreement between present velocity profiles of single-sided lid-driven cubical cavity results and those of Mei et al.[17] and Ku et al.[10] is excellent. The close agreement gives credibility to the result of present three-dimensional lattice Boltzmann code and it stands validated.

3.2 3-d two-sided lid-driven cavity flow with antiparallel wall motion

An incompressible viscous flow in a cubical cavity whose top and bottom walls move in the opposite (antiparallel motion) direction with a uniform velocity is the problem investigated in the present work. Fig.

3 shows the three-dimensional two-sided lid-driven cubical cavity flow. The results presented in this section show the accuracy and capability of the present LBM code to compute steady viscous flows. The present problem consists of a cubic cavity filled with a stationary fluid that is set into motion by the sudden movement of the top and bottom walls from the left to right. The boundary conditions for the three-dimensional two-sided cubical cavity are $u = v = w = 0$ at $x = 0$ and $x = 1$; $u = U$ at $y = 0$ and $v = w = 0$ at $y = 1$. $u = -U$ at $y = 1$ and $v = w = 0$ at $y = 1$; $u = v = w = 0$ at $z = 0$ and $z = 1$.

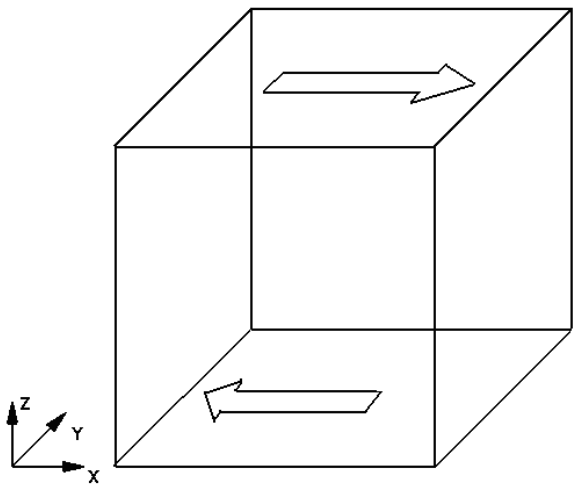

Fig. 3. 3-D Two-sided lid-driven cubical cavity with antiparallel wall motion

As has already been mentioned the flow in a three-dimensional cubical cavity with two-sided antiparallel wall movement has not been examined so far. Owing to the boundary layer effect of the side walls the three-dimensional results at mid-plane will deviate from the two-dimensional results. It may be recalled that, in steady two-dimensional flows all streamlines are closed except for streamlines that separate eddies by starting and ending on walls. It is known that, the three-dimensional streamlines do not close, not even in mid-plane even at low Re. In the present work, computations are carried out for $Re = 10, 100, 400$ and 700. Fig. 4 shows the steady-state streamline patterns obtained using a $67 \times 67 \times 67$ lattice size for $Re = 10, 100, 400$ and 700. cavity. At $Re = 10$, two primary vortices appear and they are symmetrical to each other in the form of elliptical shape. At $Re = 100$, two primary vortices merged into single primary vortex and primary vortex core move towards the centre of a geometrical domain. At $Re = 400$, the primary vortex core take position in the geometric centre of the three-dimensional two-sided cubical cavity. Fig. 4(d) showing the appearance of two secondary vortices near the top left and the bottom right corners of the cavity and a very small shift of the primary vortex centre from the geometric centre of the cavity. Beya and Lili[4] concluded that for a two-sided non-facing lid-driven cavity at $Re = 600$ the flow is not steady and periodic solution exists, whereas for the three-dimensional two-sided lid-driven cubical cavity with antiparallel motion I find that exists a unique, steady and stable solution[1, 14]. In order to distinguish between the three-dimensional and two-dimensional steady flow patterns, the two-dimensional streamline patterns shown for comparison.

Fig. 5 shows the steady-state streamline patterns for various Reynolds numbers on a 256×256 lattice size. At $Re = 10$, two primary co-rotating vortices appear in the centre of a cavity. It is also seen that, as the Reynolds number increases a single primary vortex appears at the geometric centre of the cavity. At $Re = 700$, the appearance of two secondary vortices near the top left and the bottom right corners of the cavity. As shown in Fig. 4 and Fig. 5, these results confirm that the results obtained through three-dimensional model reveal the effect of 3D with the available two-dimensional results. To understand the three-dimensional boundary effect, the velocity profiles of the component on the vertical (y-direction) centreline on the plane at $Re = 10, 100, 400$ and 700 is shown in Fig. 6. The deviation between two-dimensional and three-dimensional results though small, it is good enough to indicate that sidewall effects can be perceived at mid-span even at relatively low Reynolds numbers. It is also seen that, the discrepancy between two- and two-dimensional velocity profiles

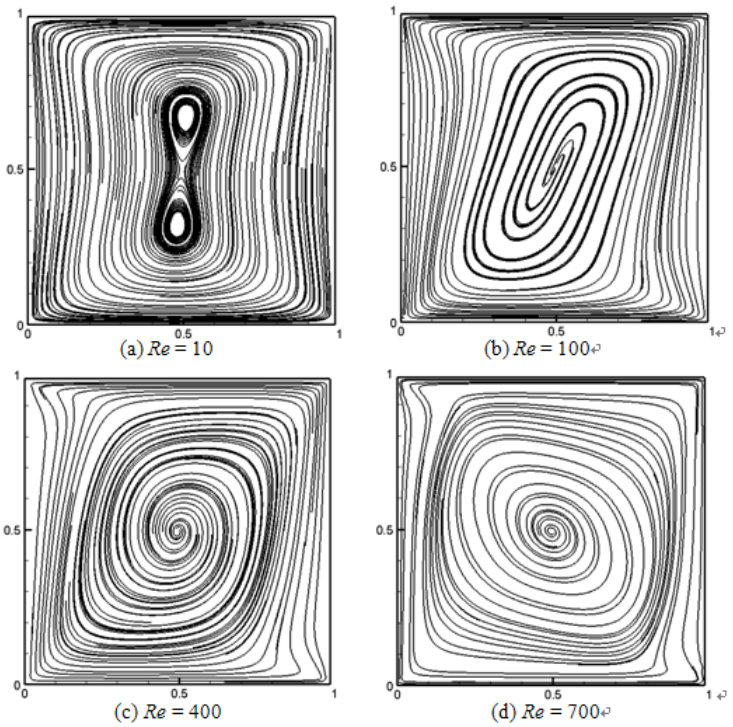

Fig. 4. Steady state streamline patterns for different Reynolds numbers for the three-dimensional two-sided cubical cavity with antiparallel wall motion

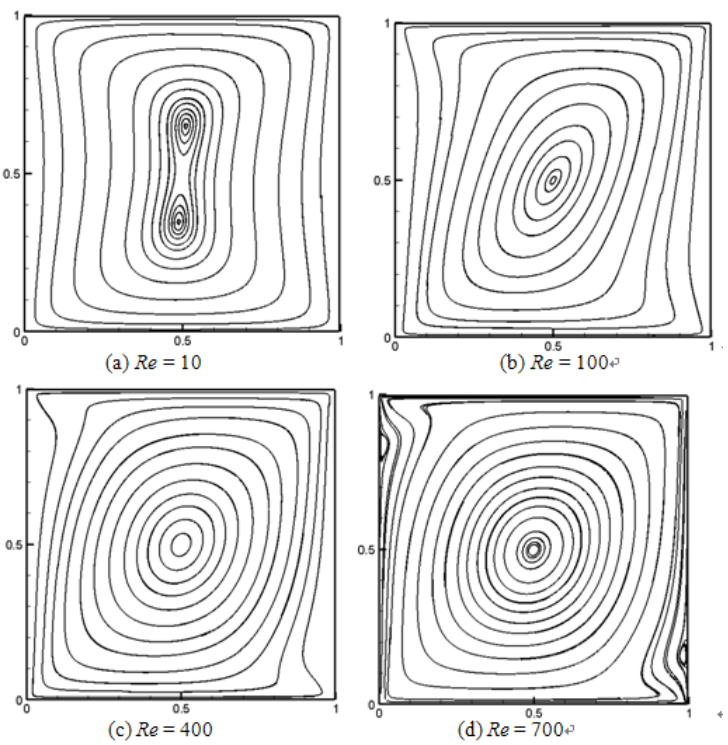

Fig. 5. Steady state streamline patterns for different Reynolds numbers for the two-dimensional two-sided square cavity

is a proof of the end-wall effect even at low Re. It is also demonstrated that three-dimensional velocities tend to be smaller than the corresponding two-dimensional values. The present LBM three-dimensional two-sided lid-driven cavity results reveal the fact that the effects of end walls are less when the Reynolds number is low. Tab. 1 gives the locations of the vortex centres for $Re = 10, 100, 400$ and 700. All these results show that the three-dimensional effect, which further substantiates the accuracy of the present 3DLBM computations.

Table 1. Locations of the vortices for antiparallel wall motion

D2Q9 Model						
Re	Primary Vortex (PV)		Secondary Vortices (SV)			
			Bottom Right(BR)		Top Left (TL)	
	x	y	x	y	x	y
10	0.332 0.656	0.332 0.656				
100	0.500	0.500				
400	0.500	0.498				
700	0.499	0.496	0.977	0.151	0.022	0.848
D3Q19 Model						
Re	Primary Vortex (PV)		Secondary Vortices (SV)			
			Bottom Right(BR)		Top Left (TL)	
	x	z	x	z	x	z
10	0.326 0.664	0.326 0.664				
100	0.499	0.498				
400	0.498	0.496				
700	0.497	0.497	0.981	0.155	0.019	0.835

3.3 3-d two-sided lid-driven cavity flow with parallel wall motion

An incompressible viscous flow in a cubical cavity whose top and bottom walls move in the same (parallel motion) direction with a uniform velocity is the problem investigated in the present work. Fig. 7 shows the three-dimensional two-sided lid-driven cubical cavity flow. The boundary conditions for the two-sided cubical cavity are $u = v = w = 0$ at $x = 0$ and $x = 1$; $u = U$ at $y = 0$ and $v = w = 0$ at $y = 1$. $u = U$ at $y = 1$ and $v = w = 0$ at $y = 1$; $u = v = w = 0$ at $z = 0$ and $z = 1$.

Fig. 8 shows the streamline patterns obtained using a $67 \times 67 \times 67$ lattice size $Re = 10, 100, 400$ and 700. Here the upper and lower walls move in the same direction along the x-axis with the same velocity. The streamlines are found to be symmetrical with respect to a line parallel to these walls and passing through the cavity centre.

At low Reynolds numbers, ($Re = 10 and 100$) two counter-rotating primary vortices symmetrical to each other are seen to form with a free shear layer in between (Fig. 8 (a) and (b)). At these Reynolds numbers the primary vortex cores are seen to be somewhat away from the centres of the top and the bottom halves of the cavity towards the righthand top and righthand bottom corners respectively. At $Re = 400$ (Fig. 8(c)), apart from the primary vortices a pair of counter-rotating secondary vortices symmetrically placed about the horizontal centreline are seen to appear near the centre of the right wall. As the Reynolds number increases (Fig. 8(d)) the secondary vortices near the centre of the right wall grow in size. The counter-rotating pairs of primary and secondary vortices maintain their symmetry at all the Reynolds numbers investigated here. From Fig. 8 it is observed that as the Reynolds number increases the cores of the primary vortices move from near the top right and bottom right corners towards the centres of the top and bottom halves of the cavity respectively. Fig. 9 shows the steady-state streamline patterns for various Reynolds numbers on a 256×256 lattice size. As shown in Fig. 8 and Fig. 9, these results confirm that the results obtained through three-dimensional model reveal the effect of 3D with the available two-dimensional results. The velocity profiles of the u component on the vertical (y-dirn) centreline on the plane $z = 0.5$ at $Re = 10, 100, 400$ and 700 is shown in Fig. 10. The discrepancy between two- and three-dimensional velocity profiles is a proof of the end-wall effect even at low Re. Tab. 2 gives the locations of the vortex centres for $Re = 10, 100, 400$ and 700.

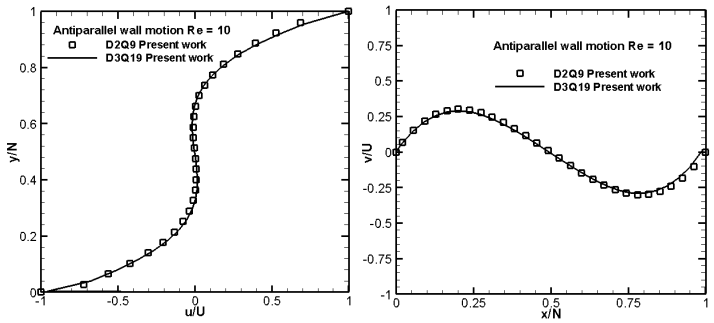

(a) Re = 10

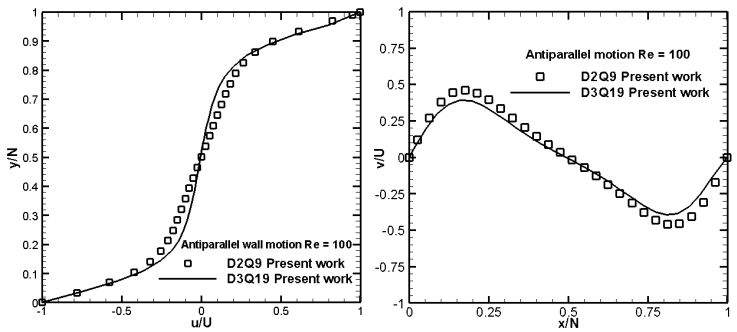

(b) Re = 100

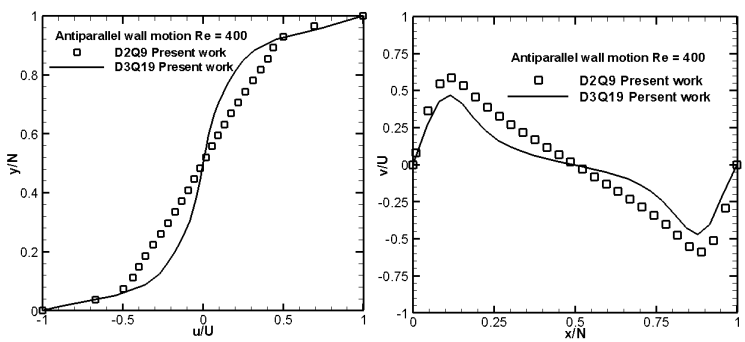

(c) Re = 400

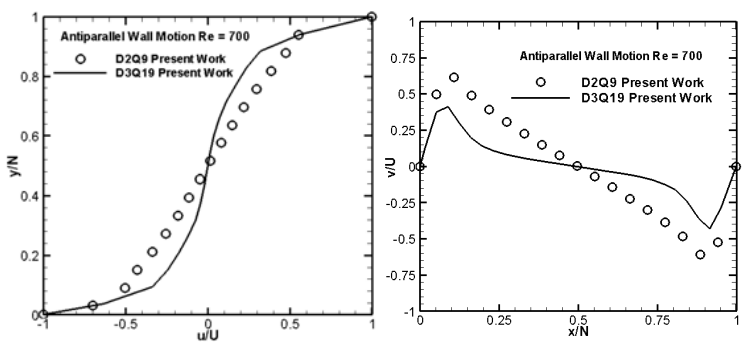

(d) Re = 700

Fig. 6. Comparison of centreline u-velocity and v-velocity of two-sided cubical and square cavity at Re = 10, 100, 400 and 700

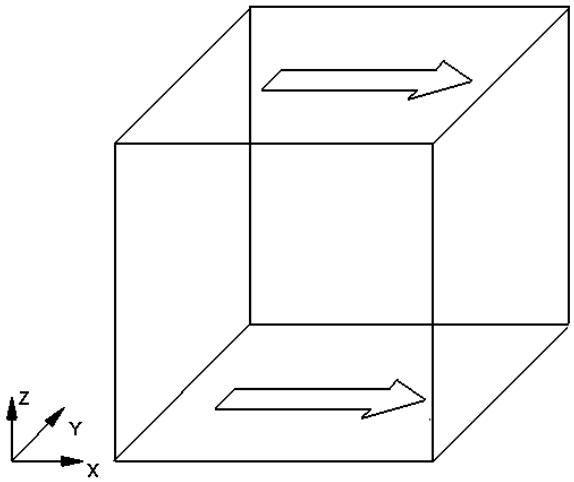

Fig. 7. 3-D Two-sided lid-driven cubical cavity with parallel wall motion

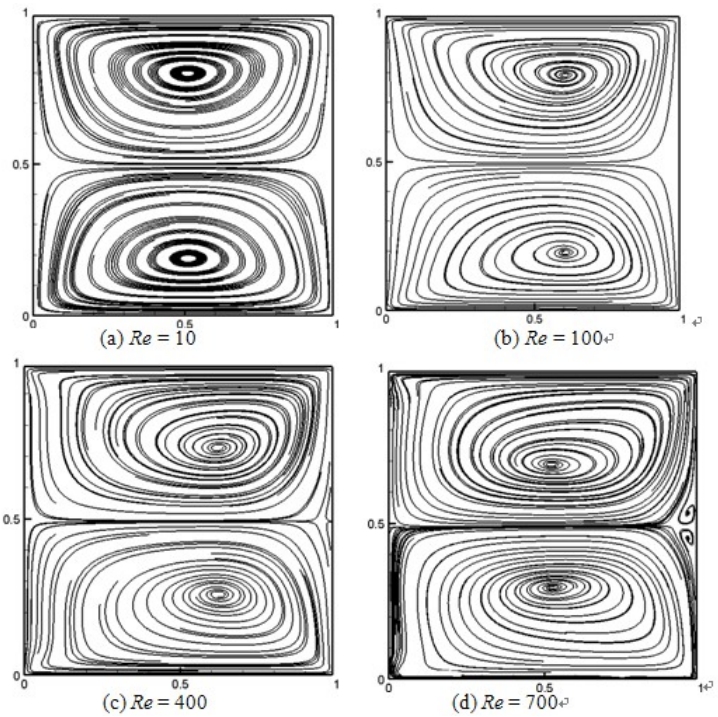

Fig. 8. Steady state streamline patterns for different Reynolds numbers for the two-sided cubical cavity with parallel wall motion

4 Conclusion

In this work a relatively unexplored flow configuration in a three-dimensional two-sided lid-driven cubical cavity is computed with the Lattice Boltzmann Method. In the case of two-dimensional anti-parallel wall motion, a single primary vortex is formed at the centre of a domain. After having used the LBM code to compute the flow in the single-sided lid-driven cubical cavity to establish its credibility, it is then used to compute steady-state flows in a hitherto unexplored configuration, namely, the two-sided cubical cavity flow induced by the motion of two facing walls in the opposite direction. In the case of three-dimensional parallel wall motion, besides two primary vortices, there also appears a pair of counter-rotating secondary vortices symmetrically placed about the centreline parallel to the motion of the walls. The code developed for the present steady state computations can also be effectively used for various other three-dimensional rectangular

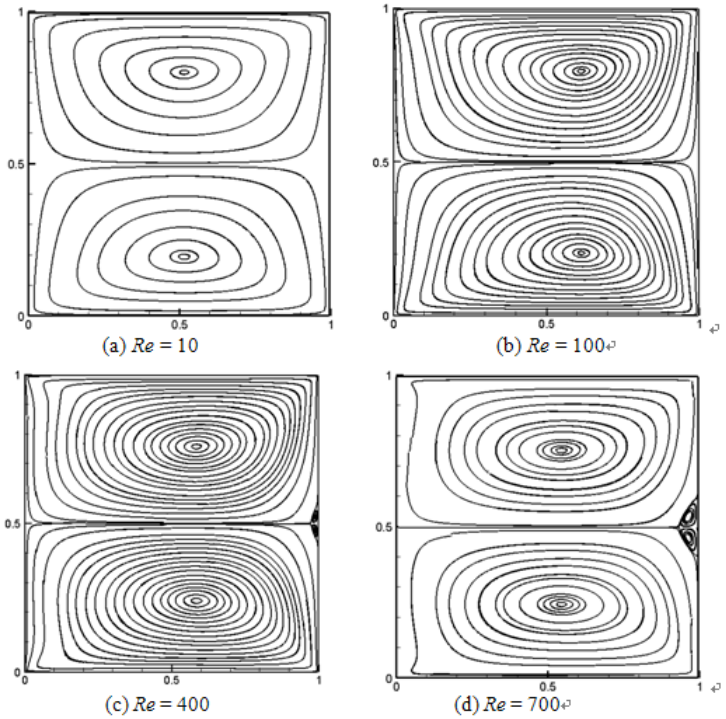

Fig. 9. Steady state streamline patterns for different Reynolds numbers for the two-dimensional two-sided square cavity

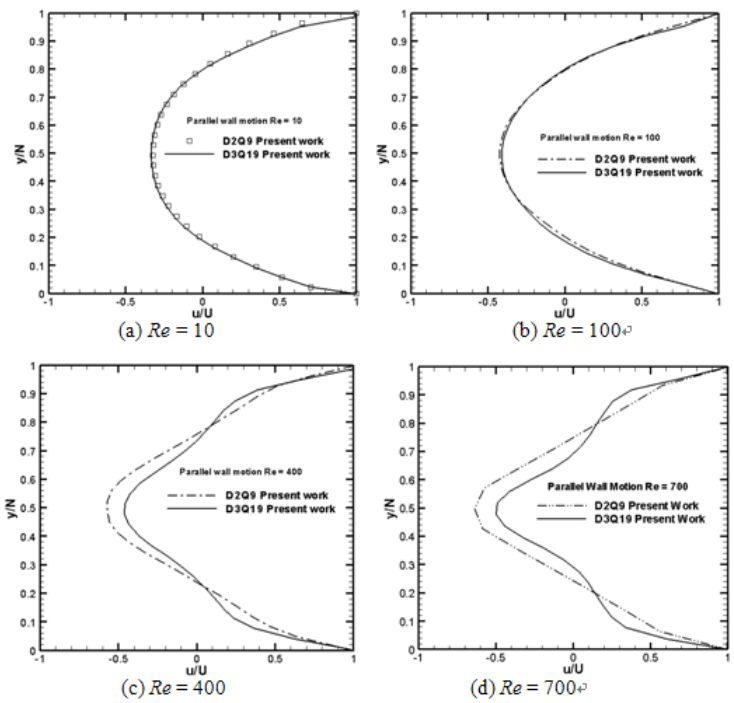

Fig. 10. Comparison of centreline u-velocity of two-sided cubical and square cavity at Re = 10, 100, 400 and 700

geometries. Overall it is seen that the present lattice Botzmann method can be used effectively to produce accurate results and capture all the flow features that conventional methods like finite volume (FV) and finite difference (FD) methods are capable of capturing.

Table 2. Locations of the vortices for parallel wall motion

D2Q9 Model								
Re	Primary Vortex Centres (PVC)				Secondary Vortex Centres (SCV)			
	Bottom		Top		Bottom		Top	
	x	y	x	y	x	y	x	y
10	0.511	0.176	0.511	0.788				
100	0.604	0.202	0.604	0.795				
400	0.594	0.238	0.594	0.755	0.987	0.463	0.987	0.526
700	0.544	0.239	0.544	0.749	0.961	0.460	0.960	0.531
D3Q19 Model								
Re	Primary Vortex Centres (PVC)				Secondary Vortex Centres (SCV)			
	Bottom		Top		Bottom Right(BR)		Top Left (TL)	
	x	z	x	z	x	z	x	z
10	0.510	0.186	0.508	0.790				
100	0.612	0.196	0.612	0.792				
400	0.602	0.242	0.602	0.726	0.986	0.456	0.986	0.520
700	0.535	0.295	0.535	0.686	0.959	0.447	0.959	0.531

5 Acknowledgement

Author thanks Dr. Anoop K.Dass, Professor, Department of Mechanical Engineering, Indian Institute of Technology Guwahati for fruitful discussions and guidance.

References

[1] D. Perumal, A. Dass. Simulation of incompressible flows in two-sided lid-driven square cavities *Part II-LBM, CFD Letters*, 2010, **2**(1): 25–38.

[2] A. Tamura, K. Okuyama, et al. Three-dimensional discrete-velocity BGK model for the incompressible Navier-Stokes equations. *Computers & Fluids*, 2011, **40**(1): 149–155.

[3] S. Albensoeder, H. Kuhlmann. Accurate three-dimensional lid-driven cavity flow. *Journal of Computational Physics*, 2005, **206**: 536–558.

[4] B. Beya, T. Lili. Three-dimensional incompressible flow in a two-sided non-facing lid-driven cubical cavity. *Comptes Rendus Mecanique*, 2008, **336**(11): 863–872.

[5] A. Cortesand, J. Miller. Numerical experiments with the lid driven cavity problem. *Computers & Fluids*, 1994, **23**: 1005–1027.

[6] A. Perumal, G. Kumar, A. Dass. Numerical simulation of viscous flow over a square cylinder using lattice Boltzmann method. *ISRN Mathematical Physics*, 2012, **2012**.

[7] D. Yu, R. Mei, et al. Viscous flow computations with the method of lattice boltzmann equation. *Progress in Aerospace Sciences*, 2003, **39**(5): 329–367.

[8] R. Du, B. Shi. Incompressible multi-relaxation-time lattice boltzmann model in 3-d space. *Journal of Hydrodynamics, Ser. B*, 2010, **22**(6): 782–787.

[9] F. Oueslati, B. Ben Beya, T. Lili. Aspect ratio effects on three-dimensional incompressible flow in a two-sided non-facing lid-driven parallelepiped cavity. *Comptes Rendus Mecanique*, 2011, **339**(10): 655–665.

[10] H. Ku, R. Hirsh, T. Taylor. A pseudospectral method for solution of the three-dimensional incompressible navier-stokes equations. *Journal of Computational Physics*, 1987, **70**(2): 439–462.

[11] J. Koseff, R. Street. Visualization studies of a shear driven three-dimensional recirculating flow. *Journal of Fluids Engineering*, 1984, **106**: 21–33.

[12] S. Mendu, P. Das. Flow of power-law fluids in a cavity driven by the motion of two facing lids-a simulation by lattice boltzmann method. *Journal of Non-Newtonian Fluid Mechanics*, 2012, **175**: 10–24.

[13] D. Perumal. Simulation of flow in two-sided lid-driven deep cavities by the finite difference method. *Journal of Applied Science in the Thermodynamics and Fluid Mechanics*, 2012, **6**(1): 1–6.

[14] D. Perumal, A. Dass. Simulation of incompressible flows in two-sided lid-driven square cavities. Part I-FDM. *CFD Letters*, 2010, **2**(1): 13–24.

[15] D. Perumal, A. Dass. Multiplicity of steady solutions in two-dimensional lid-driven cavity flows by lattice boltzmann method. *Computers & Mathematics with Applications*, 2011, **61**(12): 3711–3721.
[16] D. Perumal, A. Dass. Application of lattice boltzmann method for incompressible viscous flows. *Applied Mathematical Modelling*, 2012, **37**(6): 4075–4092.
[17] R. Mei, W. Shyy, et al. Lattice boltzmann method for 3-d flows with curved boundary. *Journal of Computational Physics*, 2000, **161**(2): 680–699.
[18] S. Hou, Q. Zou, et al. Simulation of cavity flow by the lattice boltzmann method. *Journal of Computational Physics*, 1995, **118**(2): 329–347.
[19] P. Shankar, M. Deshpande. Fluid mechanics in the driven cavity. *Annual Review of Fluid Mechanics*, 2000, **32**(1): 93–136.
[20] T. Shew, S. Tsai. Flow topology in a steady three-dimensional lid-driven cavity. *Computers & Fluids*, 2002, **31**(911-934).
[21] J. Wu, C. Shu. An improved immersed boundary-lattice boltzmann method for simulating three-dimensional incompressible flows. *Journal of Computational Physics*, 2010, **229**(13): 5022–5042.